

# A study of $\lambda$ Bootis type stars in the wavelength region beyond 7000 Å<sup>\*</sup>

E. Paunzen<sup>1,2</sup>, I. Kamp<sup>3</sup>, W.W. Weiss<sup>1</sup>, H. Wiesemeyer<sup>4</sup>

<sup>1</sup> Institut für Astronomie der Universität Wien, Türkenschanzstr. 17, A-1180 Wien, Austria  
e-mail: ernst.paunzen@univie.ac.at, weiss@astro.univie.ac.at

<sup>2</sup> Zentraler Informatikdienst der Universität Wien, Universitätsstr. 7, A-1010 Wien, Austria

<sup>3</sup> Leiden Observatory, Niels Bohrweg 2, PO Box 9513, 2330 RA Leiden, The Netherlands  
e-mail: kamp@strw.leidenuniv.nl

<sup>4</sup> IRAM Grenoble, 300 Rue de la Piscine, Domaine Universitaire, F-38406 St. Martin d'Hères Cedex, France  
e-mail: wiesemey@iram.fr

Received 2002; accepted 2003

**Abstract.** The group of  $\lambda$  Bootis type stars comprises late B- to early F-type, Population I objects which are basically metal weak, in particular the Fe group elements, but with the clear exception of C, N, O and S. One of the theories to explain the abundance pattern of these stars involves circumstellar or interstellar matter around the objects. Hence, we have compiled all available data from the literature of well established members of the  $\lambda$  Bootis group redward of 7000 Å in order to find evidence for matter around these objects. Furthermore, we present unpublished ISO as well as submillimeter continuum and CO (2 – 1) line measurements to complete the data set. In total, measurements for 34 (26 with data redward of 20  $\mu$ m) well established  $\lambda$  Bootis stars are available. There is evidence for an infrared excesses in six stars (HD 31295, HD 74873, HD 110411, HD 125162, HD 198160/1 and HD 210111) and two are doubtful cases (HD 11413 and HD 192640) resulting in a percentage of 23 % (excluding the two doubtful cases). Dust models for these objects show fractional dust luminosities comparable to the Vega-type stars and slightly higher dust temperatures. ISO-SWS spectroscopy for HD 125162 and HD 192640 resulted in the detection of pure stellar H I lines ruling out an active accretion disk (as found for several Herbig Ae/Be stars) around these objects. The submillimeter measurements gave only upper limits for the line and continuum fluxes.

**Key words.** Stars:  $\lambda$  Bootis – chemically peculiar – early-type

## 1. Introduction

The group of  $\lambda$  Bootis stars comprise of true Population I, late B to early F-type stars, with moderate to extreme (up to a factor 100) surface underabundances of most Fe-peak elements and solar abundances of lighter elements (C, N, O, and S). Only a maximum of about 2% of all objects in the relevant spectral domain are believed to be  $\lambda$  Bootis type stars (Paunzen 2001, Gray & Corbally 2002).

One of the most promising theories explaining the  $\lambda$  Bootis phenomenon is the diffusion/accretion theory (Turcotte & Charbonneau 1993, Andrievsky & Paunzen 2000, Kamp & Paunzen 2002, Turcotte 2002). Within

this model, interstellar or circumstellar gas is accreted by the star. Hence, a circumstellar disk or shell should exist around  $\lambda$  Bootis stars which manifests itself in an infrared (IR hereafter) excess.

The first near-infrared data for well established  $\lambda$  Bootis stars was already published by Oke (1967). He lists spectrophotometry for HD 31295, HD 125162 and HD 192640 up to 10870 Å. Data for wavelengths beyond 10  $\mu$ m became available with the launch of the IRAS-satellite. The IR excesses detected for Vega,  $\epsilon$  Eridani,  $\alpha$  Piscis Austrini and  $\beta$  Pictoris (Aumann et al. 1984) have been interpreted as due to cold circumstellar disks or shells around these stars. Later, the disk of  $\beta$  Pictoris was directly imaged in the IR revealing a solar system-sized dust disk extending to at least 1100 AU (Smith & Terrile 1984). A simple model of this system indicates a central star (spectral type: A5V), encircled by an ionized gaseous inner disk and an outer dust disk. Aumann (1985) established the group of Vega-like stars containing main-sequence (MS

*Send offprint requests to:* E. Paunzen

\* Based on observations with ISO, an ESA project with instruments funded by ESA Member States (especially the PI countries: France, Germany, the Netherlands and the United Kingdom) and with the participation of ISAS and NASA; and observations at the Heinrich-Hertz-Telescope (HHT, operated by the the Submillimeter Telescope Observatory).

**Table 1.** Presence of infrared excess and/or narrow absorption lines towards the well established, apparent single type  $\lambda$  Bootis stars. A question mark indicates doubtful cases. The projected rotational velocities were taken from Paunzen et al. (2002). We have indicated the origin of gas features either as interstellar (IS) or circumstellar (CS) from the literature as listed in Sect. 2.2.1.

HD	HR	IRAS	dust	gas	$v \sin i$
11413	541	F01489–5027	y?	CS?	125
31295	1570	04521+1004	y		115
74873	3481	F08441+1217	y		130
110411	4828	12394+1030	y		165
125162	5351	14144+4619	y	CS?	115
142994				CS	180
183324	7400			CS?	90
192640	7736	20126+3639	y?	IS	80
193256	7764C			IS	250
193281	7764A	F20173–2921		IS	95
198160	7959	F20474–6237	y	CS?	200
210111	8437	F22058–3322	y		55
221756	8947	23321+3957	y	CS	105

hereafter) stars also showing an infrared excess (defined by the IRAS colors at 12 and 60  $\mu\text{m}$ :  $[12] - [60] > 1 \text{ mag}$ ) similar to the prototype Vega. Many Vega-like stars are in fact much cooler than Vega (A0 V) itself.

Several papers (Gerbaldi 1991, King 1994, Andriolat et al. 1995) were devoted to the group of  $\lambda$  Bootis stars presenting data in the IR wavelength region but none of them presented a comprehensive analysis of all available data. Furthermore, the ISO satellite brought a flood of new data for group members. Fajardo-Acosta et al. (1999) presented data for three  $\lambda$  Bootis stars, namely HD 11413, HD 110411 and HD 192640.

In Sect. 2, we summarize the current literature status on the  $\lambda$  Bootis phenomenon focusing especially on circumstellar dust and gas. We have reanalyzed in Sect. 3 all available measurements in the wavelength range beyond 7000 Å, using the newest available calibrations (especially important for ISO measurements) and present data for 36 well established  $\lambda$  Bootis stars. This starting wavelength was chosen such that a good estimate for fitting a black-body radiation curve could be made. The final goal of this work is to derive the incidence of objects with IR excess and to compare the observed fluxes for  $\lambda$  Bootis type objects with those of models to derive first estimates for the dust temperature and the optical depth of the circumstellar and/or interstellar material (Sect. 4).

## 2. The $\lambda$ Bootis phenomenon and observations in the IR-region

In principle, three models were developed to explain the  $\lambda$  Bootis phenomenon: 1) the diffusion/mass-loss; 2) the diffusion/accretion and 3) the binarity model. Since the second model is the one relevant for this paper, we describe the other two just briefly.

The diffusion/mass-loss theory was formulated by Michaud & Charland (1986). They modified the highly successful diffusion model for the AmFm phenomenon in order to account for stellar mass-loss. AmFm stars are Population I, nonmagnetic MS stars with underabundances of Ca and Sc, but large overabundances of most heavier elements (up to a factor of 500). This abundance pattern is explained by gravitational settling of He which leads to the disappearance of the outer convection zone associated with He-ionization. Later, Charbonneau (1993) showed that (at any time of the MS evolution) even moderate equatorial rotational velocities of 50  $\text{km s}^{-1}$  seem to prevent the appearance of the underabundance pattern, because meridional circulation effectively mixes the stellar atmosphere. Beside the estimation of stellar ages for members of the  $\lambda$  Bootis group, so far no other observational tests are suggested for this model.

The binarity theory explains the apparent spectral peculiarities either by undetected spectroscopic binary systems (Faraggiana & Bonifacio 1999) or by a single type object which is a product of a merging process similar to blue stragglers (Andrievsky 1997). Both approaches can only account for the nature of a small number of objects. Faraggiana et al. (2001) and Marchetti et al. (2001) failed to detect any new spectroscopic binary system among their observed sample. Iliev et al. (2002) reported about two spectroscopic binary systems, which comprise only  $\lambda$  Bootis type objects.

The diffusion/accretion model is so far the most promising theory in order to explain the  $\lambda$  Bootis phenomenon. Venn & Lambert (1990) were the first who noticed the similarity between the abundance pattern of  $\lambda$  Bootis stars and the depletion pattern of the interstellar medium (ISM) and suggested the accretion of interstellar or circumstellar gas to explain the  $\lambda$  Bootis stars. In the ISM metals are underabundant because of their incorporation in dust grains or ice mantles around the dust grains.

Following this, Waters et al. (1992) worked out a scenario, where the  $\lambda$  Bootis star accretes metal-depleted gas from a surrounding disk. In this model, the dust grains are blown away by radiation pressure and coupling between dust and gas is negligible. Considering the spectral-type of  $\lambda$  Bootis stars, the gas in the disk remains neutral and hence does not experience significant direct radiation pressure.

Turcotte & Charbonneau (1993) calculated the abundance evolution in the outer layers of a  $\lambda$  Bootis star assuming accretion rates between  $10^{-15}$  and  $10^{-12} M_{\odot} \text{ yr}^{-1}$ . Solving the diffusion equation modified this time by an additional accretion term, they obtained the time evolution of the Ca and Ti abundance stratification with and without stellar rotation. From their calculations, a lower limit of  $10^{-14} M_{\odot} \text{ yr}^{-1}$  is derived for the diffusion/accretion model to produce a typical  $\lambda$  Bootis abundance pattern.



Table 2. continued.

System	$\lambda_c$ [ $\mu\text{m}$ ]	125162	125889	142703	142994	149130	156954	168740	170680	183324
J(R)	0.7	62.2(3.1)	–	–	–	–	–	–	–	–
13c	0.7241	65.1(3.3)	–	–	–	–	–	–	–	–
13c	0.8	58.2(2.9)	–	–	–	–	–	–	–	–
13c	0.8584	55.5(2.8)	–	–	–	–	–	–	–	–
J(I)	0.9	50.1(2.5)	–	–	–	–	–	–	–	–
13c	0.9831	55.0(2.8)	–	–	–	–	–	–	–	–
Oke	0.995	53.3(2.7)	–	–	–	–	–	–	–	–
Oke	1.0256	51.3(2.6)	–	–	–	–	–	–	–	–
Oke	1.04	51.8(2.6)	–	–	–	–	–	–	–	–
Oke	1.061	–	–	–	–	–	–	–	–	–
Oke	1.0796	49.5(2.5)	–	–	–	–	–	–	–	–
Oke	1.087	–	–	–	–	–	–	–	–	–
13c	1.1084	48.5(2.4)	–	–	–	–	–	–	–	–
J(J)	1.25	42.1(7)	0.33(1)	–	–	–	2.41(1)	–	–	–
J(H)	1.65	28.1(6)	0.26(1)	–	–	–	1.84(1)	–	–	–
J(K)	2.2	17.9(8)	0.18(1)	5.24(3)	–	–	1.27(1)	–	–	–
ISO P1(C)	3.29	–	–	–	–	–	–	–	–	–
ISO P1(C)	3.6	–	–	3.07(88)	–	–	–	–	–	–
ISO P1(S)	3.6	–	–	–	0.87	–	–	–	–	–
J(L)	3.8	–	–	–	–	–	–	–	–	–
J(M)	4.7	–	–	–	–	–	–	–	–	–
ISO P1(C)	4.85	4.30(34)	–	1.54(53)	–	–	–	–	–	–
ISO P1(C)	11.5	1.82(23)	–	0.56(26)	–	–	–	–	–	–
ISO P1(S)	11.5	–	–	–	2.72	–	–	–	–	–
IRAS	12	0.79(8)	–	0.23(4)	–	0.25(5)	–	0.18(3)	0.25(5)	–
ISO P2(C)	20	–	–	0.22(13)	–	–	–	–	–	0.17(11)
ISO P2(S)	20	0.62	–	–	2.45	–	–	–	–	–
IRAS	25	0.26(4)	–	0.09	–	0.07(2)	–	0.06	0.31	–
ISO P2(C)	25	–	–	–	–	–	–	–	–	–
IRAS	60	0.25(5)	–	0.02	–	0.01	–	0.08	0.08	–
ISO P3(S)	60	–	–	–	1.02	–	–	–	–	–
ISO C1(C)	60	–	–	–	–	–	–	–	–	0.02(6)
IRAS	100	0.59	–	0.33	–	2.25	–	0.66	1.95	–
ISO P3(C)	100	0.22(7)	–	–	–	–	–	–	–	–
System	$\lambda_c$ [ $\mu\text{m}$ ]	192640	193256	193281	198160	204041	210111	221756		
J(R)	0.7	36.1(1.8)	–	–	–	–	–	16.6(8)	–	–
13c	0.7241	33.2(1.7)	–	–	–	–	–	–	–	–
13c	0.8	31.2(1.6)	–	–	–	–	–	–	–	–
13c	0.8584	29.3(1.5)	–	–	–	–	–	–	–	–
J(I)	0.9	30.2(1.5)	–	–	–	–	–	15.4(8)	–	–
13c	0.9831	29.2(1.5)	–	–	–	–	–	–	–	–
Oke	0.995	32.4(1.6)	–	–	–	–	–	–	–	–
Oke	1.0256	32.7(1.6)	–	–	–	–	–	–	–	–
Oke	1.04	31.5(1.6)	–	–	–	–	–	–	–	–
Oke	1.061	33.0(1.7)	–	–	–	–	–	–	–	–
Oke	1.0796	31.5(1.6)	–	–	–	–	–	–	–	–
Oke	1.087	33.6(1.7)	–	–	–	–	–	–	–	–
13c	1.1084	26.5(1.3)	–	–	–	–	–	–	–	–
J(J)	1.25	23.1(1.2)	2.04(1)	5.61(4)	–	–	–	–	–	–
J(H)	1.65	16.8(8)	1.51(1)	4.80(6)	–	–	–	–	–	–
J(K)	2.2	10.4(5)	1.05(1)	3.26(5)	–	–	–	–	–	–
ISO P1(C)	3.29	–	–	–	–	–	–	2.11(63)	–	–
ISO P1(C)	3.6	–	–	–	–	1.23(55)	–	–	–	–
ISO P1(S)	3.6	3.86(15)	1.38(3)	–	3.54(11)	–	1.20(2)	2.36(2)	–	–
J(L)	3.8	3.97(20)	–	–	–	–	–	–	–	–
J(M)	4.7	2.44(12)	–	–	–	–	–	–	–	–
ISO P1(C)	4.85	1.79(71)	–	–	–	1.17(50)	–	0.91(43)	–	–
ISO P1(C)	11.5	–	–	–	–	0.26(19)	–	–	–	–
ISO P1(S)	11.5	0.37(3)	0.03	–	0.39(6)	–	0.17(3)	0.69(6)	–	–
IRAS	12	0.44(8)	0.23(4)	–	0.25(5)	0.10(2)	0.17(3)	0.24(5)	–	–
ISO P2(C)	20	–	–	–	–	0.07(24)	–	–	–	–
ISO P2(S)	20	0.19(13)	0.31(13)	–	0.27(12)	–	0.25(14)	0.08(13)	–	–
IRAS	25	0.18	0.11	–	0.18	0.09	0.06	0.06(3)	–	–
ISO P2(C)	25	0.20(28)	–	–	–	0.02(3)	–	0.08(5)	–	–
IRAS	60	1.82	0.04	–	0.20	0.04	0.08	0.11	–	–
ISO P3(S)	60	–	–	–	–	–	–	–	–	–
ISO C1(C)	60	–	–	–	0.31(13)	–	0.10(7)	0.17(8)	–	–
IRAS	100	43.58	0.80	–	0.67	0.26	0.17	0.62	–	–
ISO P3(C)	100	–	–	–	–	–	–	0.01(51)	–	–

Moreover their rotating models provide evidence that meridional circulation cannot destroy the established accretion pattern for rotational velocities below  $125 \text{ km s}^{-1}$ . Since diffusion wipes out any accretion pattern within  $10^6 \text{ yr}$  at the end of accretion large number of  $\lambda$  Bootis stars should show observational evidence for the presence of circumstellar material.

The scenarios discussed above imply a constraint on the evolutionary status of the star, because the existence of a disk or a shell has to be explained in the context of stellar evolution. Circumstellar disks are thought to exist during the pre-main-sequence phase of stellar evolution, while a shell can either occur in a very early phase of pre-main-sequence evolution or after a stellar merger.

Kamp & Paunzen (2002) proposed only recently a slightly different accretion scenario for the  $\lambda$  Bootis stars, namely the accretion from a diffuse interstellar cloud. This scenario works at any stage of stellar evolution as soon as the star passes a diffuse interstellar cloud. The interstellar dust grains are blown away by the stellar radiation pressure, while the depleted interstellar gas is accreted onto the star. Typical gas accretion rates are between  $10^{-14}$  and  $10^{-10} \text{ M}_{\odot} \text{ yr}^{-1}$  depending on the density of the diffuse cloud and the relative velocity between star and cloud.

Any accretion scenario for  $\lambda$  Bootis stars involves dust grains as a mean to deplete certain metals in the gas phase. Moreover due to the short timescales of mixing, gas accretion is supposed to be ongoing in most cases. Hence, in the framework of the diffusion/accretion model a search for the infrared emission from this circumstellar or interstellar dust as well as for narrow gaseous circumstellar or interstellar lines seems promising. Furthermore the detection of such characteristics might lead to the confirmation of the diffusion/accretion model and put further constraints on its details.

### 2.1. Results of infrared measurements from the literature

The definition of the infrared region is already quite problematic. We follow the classical definition of the near-IR (7000 Å to  $1 \mu\text{m}$ ) and IR ( $1 \mu\text{m}$  to  $100 \mu\text{m}$ ) as given by Jaschek & Jaschek (1987). We have divided the already published results in signs of dust or gas around bona-fide  $\lambda$  Bootis stars. We have not included results for objects which were probably misclassified as  $\lambda$  Bootis stars (see Paunzen 2001). In the following, two objects are discussed, whose nature is rather contrary: HD 38545 and HD 111786. Both objects were classified as  $\lambda$  Bootis type by Gray (1988). HD 38545 was found to be a close binary system (see Marchetti et al. 2001 for all references). However, Faraggiana et al. (2001) were not able to decide if the found “shell” features (see Section 2.2) are due to an apparent spectroscopic binary nature or due to circumstellar gas. The same is true for HD 111786 for which Faraggiana et al. (1997) reported a spectroscopic binary nature based on IUE data. Later, Faraggiana et al. (2001)

speculated that a “clump” of at least five objects mimics one spectrum. Since we have chosen to present only well established  $\lambda$  Bootis objects, the already published results for HD 38545 and HD 111786 will be mentioned in the following Sections but they are not included in our sample of investigated objects.

#### 2.1.1. Dust around $\lambda$ Bootis stars

Sadakane & Nishida (1986) found an infrared excess for two  $\lambda$  Bootis stars, namely HD 31295 and HD 125162, from a cross correlation of the IRAS Faint Source Catalogue and the Bright Star Catalogue. King (1994) searched the IRAS catalogues for infrared detections of  $\lambda$  Bootis stars from the catalogue by Renson et al. (1990). He found that only two well established  $\lambda$  Bootis stars (HD 31295 and HD 125162) show an excess in at least one IRAS band. Moreover he concluded that the minimum gas mass necessary to cause the peculiar abundance pattern in  $\lambda$  Bootis stars is so low, that the associated dust mass  $\sim 10^{-7} \text{ M}_{\odot}$  may even be below the detection limit of IRAS or submillimeter telescopes.

Cheng et al. (1992) report the detection of an infrared excess for the  $\lambda$  Bootis star HD 110411 based on the IRAS Faint Source Catalogue. The colours of the excess are similar to those of Vega. Note that King (1994) did not confirm the infrared excess for HD 110411.

Using ISOPHOT data from the Infrared Space Observatory (ISO; Kessler et al. 1996) Fajardo-Acosta et al. (1999) confirmed the infrared excess of HD 110411 and report a tentative detection of HD 192640 (only at  $20 \mu\text{m}$ ).

The infrared excess for Vega, an object closely connected to the  $\lambda$  Bootis group, has been analyzed in more detail. The disk as seen by IRAS has a FWHM of  $30''$  (Aumann 1991) corresponding to a disk radius of  $\sim 115 \text{ AU}$ . Heinrichsen et al. (1998) observed Vega with the ISOPHOT instrument on board of the ISO satellite and found that the disk is resolved at 60 and  $90 \mu\text{m}$  yielding a FWHM of 22 and  $36''$  respectively. The disk is, as the star (Gulliver et al. 1994), seen pole-on. Submillimeter images of Vega reveal an offset of  $9''$  with respect to the stars position and a FWHM of  $24 \times 21''$  (Holland et al. 1998). Assuming typical grain sizes for fitting the infrared excess, Ciardi et al. (2001) using the Palomar Testbed Interferometer found tentative evidence for a disk inside 4 AU contributing about 5 % of the flux at  $2.2 \mu\text{m}$ .

It is still difficult to answer the question whether circumstellar dust is a basic characteristic of  $\lambda$  Bootis stars or just as frequent or rare as for all other A-type stars. The general problem is that in most cases the detectors lack the sensitivity to detect the stellar atmospheres at infrared wavelength. This makes it difficult to exclude an infrared excess in the case of a non-detection.

Habing et al. (2001) overcame this problem by choosing bright stars for which even the photosphere was detectable with the ISOPHOT instrument at  $60 \mu\text{m}$ . Hence a pure photospheric detection ruled out any dust infrared

excess. In this way they concluded that 6 out of their 15 A-type stars have circumstellar dust and that these are mostly the younger ones between 200 and 400 Myr (post-main-sequence tracks were used to determine the stellar age of the A-type stars). The general conclusion is that most stars arrive at the main-sequence surrounded by a disk which then disappears within about 400 Myr.

Dunkin et al. (1997) and Kamp et al. (2002) studied the abundance pattern in a sample of dusty A stars. Their results clearly show that the presence of dust around A-type stars does not necessarily imply the presence of the typical  $\lambda$  Bootis abundance pattern.

## 2.2. Gas around $\lambda$ Bootis stars

If the inclination of a circumstellar disk is favourable or if a star is surrounded by a shell, narrow absorption cores can be observed on top of the stellar spectrum. These arise from the additional absorption due to circumstellar material. Similar narrow absorption lines can form in the interstellar medium between the observer and the star. The most commonly observed lines are Ca II K and Na I D.

There are different criteria to distinguish between circumstellar and interstellar origin. The doublet line ratio of Na for example is a measure of the optical thickness of the absorbing medium. If the lines are optically thin, the ratio is 2.0, while it decreases to 1.0 in the case of fully saturated lines (see e.g. Spitzer 1968). Moreover an equivalent width ratio  $W(\text{Ca II})/W(\text{Na I})$  much larger than 1.0 points towards a circumstellar origin (Lagrange-Henri et al. 1990).

However, the detection of narrow gaseous circumstellar or interstellar lines (often denoted as “shell” signs) seriously questions the spectral classification criteria of the  $\lambda$  Bootis group as established by Gray (1988). He *explicitly excluded* classical shell stars from the group of  $\lambda$  Bootis stars. Let us recall the definition of a classical shell star (Jaschek & Jaschek 1987): a B/A type shell star is characterized by the simultaneous presence of 1) broad absorption lines and 2) sharp absorption lines which arise from ground states or metastable levels. The number of lines often suggests the spectrum of a supergiant with an apparent weakness of the Mg II 4481 and Si II 4128-30 lines. But the hydrogen and helium lines clearly point at a luminosity class V classification. Abt & Moyd (1973) and Jaschek et al. (1988) found that the strength of shell lines (mostly Ca II, Ti II, Fe II and Sc II) vary in time. Usually, sharp absorption features were detected in Ca II K, but only marginal absorption features in the hydrogen lines. The latter are exactly the characteristics detected for members of the  $\lambda$  Bootis group (Section 2.2.1). But Heiter (2002) showed that the classical shell stars do not share the typical abundance pattern of the  $\lambda$  Bootis group. The detection of shell features does, therefore, *not a-priori exclude* an object as being member of the  $\lambda$  Bootis group.

### 2.2.1. Confrontation with observations

*HD 11413* and *HD 198160/1*: Holweger & Rentzsch-Holm (1995) found narrow absorption cores in Ca II K for these objects. The presence of these features is correlated with stellar properties like gravity and rotational velocity indicating a circumstellar rather than interstellar origin.

*HD 38545*: Bohlender & Walker (1994) report the detection of a circumstellar shell around HD 38545 from narrow absorption features in Fe II, Ti II, Ca II and the Balmer lines. Hauck et al. (1995, 1998) found evidence for circumstellar shell features in the Ca II K line for nine candidate  $\lambda$  Bootis stars and they confirm the circumstellar shell. They use Crutcher’s formula (Crutcher 1982) to derive the velocity component of the ISM in the direction of the star and conclude that their features are clearly circumstellar. Grady et al. (1996) confirmed the detection of shell lines in the spectrum and announced the first detection of accreting circumstellar gas in a  $\lambda$  Bootis star. They observed redshifted narrow absorption components of Fe II and Zn II in the mid-ultraviolet resembling those regularly observed in the spectrum of  $\beta$  Pictoris. Kamp et al. (2002) noted the variability of the narrow absorption feature as well as an equivalent width ratio  $W(\text{Ca II})/W(\text{Na I})$  below unity. The variability underlines the presence of circumstellar gas. McAlister et al. (1993) and Marchetti et al. (2001) reported the detection of a close companion of HD 38545 using speckle interferometry.

*HD 39283*, *HD 84948*, *HD 98353*, *HD 125162*, *HD 183324* and *HD 217782*: Andriolat et al. (1995) examined a sample of 20 candidate  $\lambda$  Bootis stars in the near-IR spectral region and found that HD 39283, HD 84948, HD 98353, and HD 217782 exhibit evidence of circumstellar shells. The spectra show clear signatures of shells as seen in classical A-type shell stars. Three objects (HD 39283, HD 98353 and HD 217782) have been excluded from the  $\lambda$  Bootis group because they do not share the typical characteristics (Gray & Garrison 1987, Faraggiana et al. 1990). HD 84948 was later found to be a spectroscopic binary system (Iliev et al. 2002). The shell evidence for HD 125162 and HD 183324 is still dubious. Note that Bohlender et al. (1999) do not confirm the detection of circumstellar gas in HD 183324.

*HD 111786*: Gray (1988) was the first to notice a weak narrow absorption core in the Ca II K line of HD 111786, which he suspected to be of circumstellar origin. Holweger & Stürenburg (1991) report the presence of narrow absorption components in the Na I D and Ca II K lines. The ratio of the two Na I D lines is found to be  $\sim 1.3$ , hence a larger optical depth. This star turned out to be in fact a spectroscopic binary consisting of a broad-lined  $\lambda$  Bootis star and a narrow-lined F-type star (Faraggiana et al. 1997). Holweger et al. (1999) Ca II K. They argue that the Ca K feature seen can not be produced by the binary nature of this star, that is by the superposition of a  $\lambda$  Bootis star and an early F star. Moreover the strong variability of this feature seems to eliminate an interstellar origin. For HD 111786, the equivalent width ratio  $W(\text{Ca II})/W(\text{Na I})$

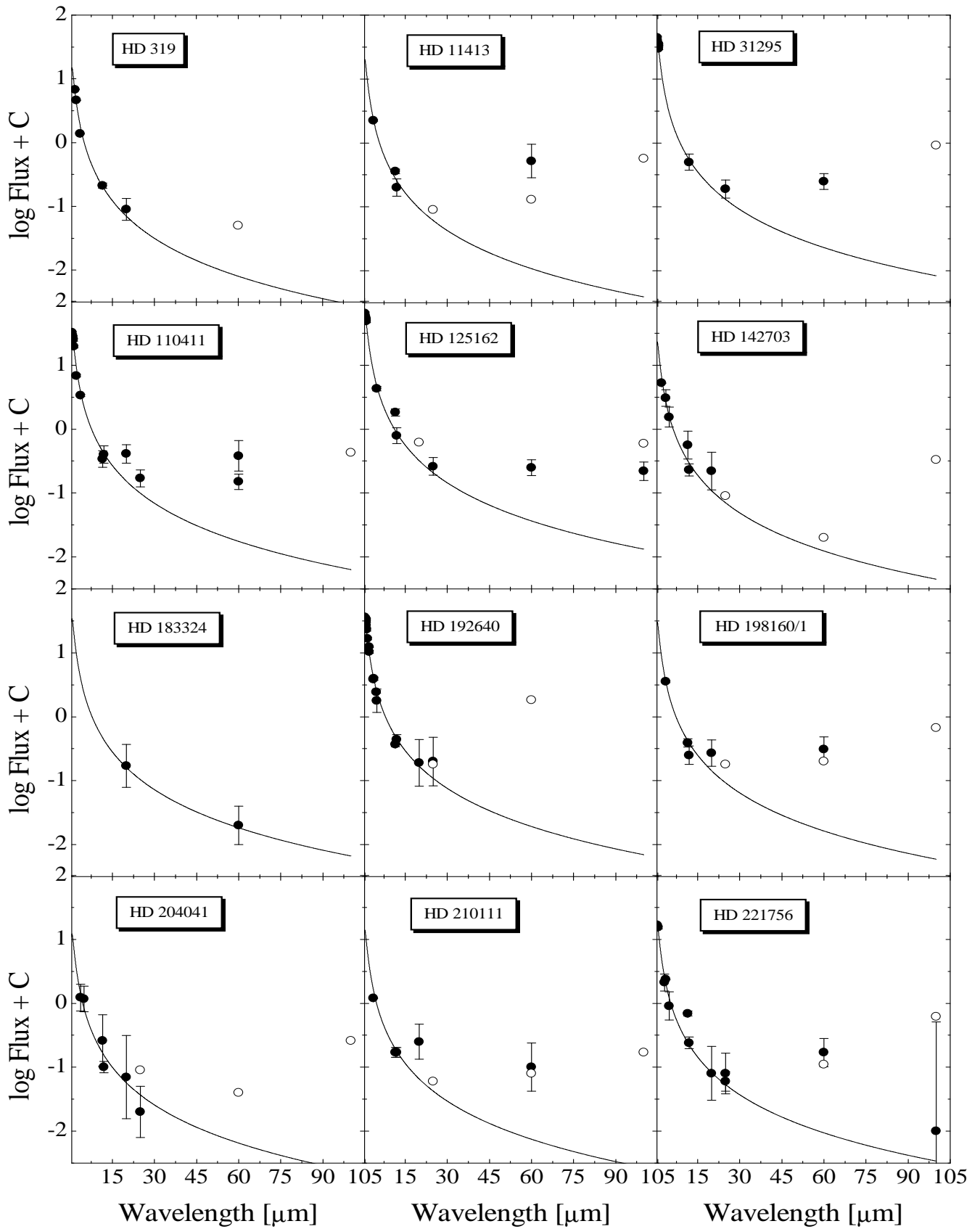


**Fig. 1.** Fluxes taken from Table 2 for HD 319, HD 11413, HD 31295, HD 110411, HD 125162, HD 142703, HD 183324, HD 192640, HD 198160/1, HD 204041, HD 210111 and HD 221756 with the blackbody curve  $T_{\text{eff}} = 8500 \text{ K}$ ; open circles are upper limits.

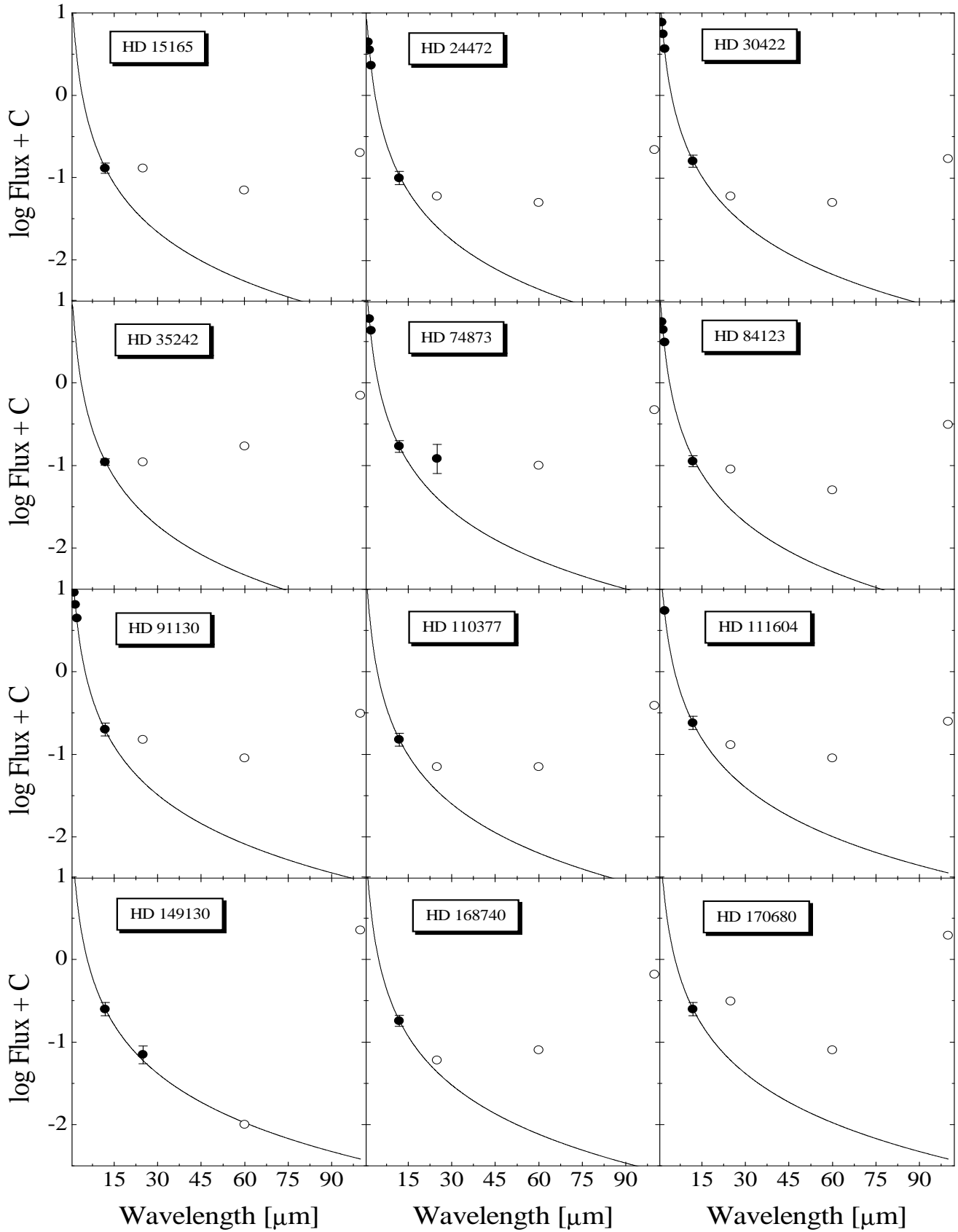


**Fig. 2.** Fluxes taken from Table 2 for HD 15165, HD 24472, HD 30422, HD 35242, HD 74873, HD 84123, HD 91130, HD 110377, HD 111604, HD 149130, HD 168740 and HD 170680 with the blackbody curve  $T_{\text{eff}} = 8500$  K; open circles are upper limits.



could be determined and was found to be about unity. The equivalent width criterium should not be taken too strict, because a range of different ionisation conditions or elemental abundances in the circumstellar gas leads to deviations from  $W(\text{CaII})/W(\text{NaI}) \gg 1$ .

*HD 142994*, *HD 192640* and *HD 221756*: Bohlender et al. (1999) reported the possible detection of strong circumstellar Na I D features in the spectra of HD 142994 and HD 221756. Moreover they note the presence of a most likely interstellar feature in HD 192640.

*HD 193256* and *HD 193281*: Holweger & Stürenburg (1991) report the presence of narrow absorption components in the Na I D and Ca II K lines for HD 193256 and HD 193281. The ratio of the two Na I D lines is found to be  $\sim 2.0$ , a possible indication for their interstellar origin. The results for HD 193256 was later confirmed by Holweger & Rentzsch-Holm (1995). Bohlender et al. (1999) cautioned against a circumstellar origin of the narrow absorption features in HD 193256 and HD 193281.

To summarize, there is definitely evidence for circumstellar gas around some  $\lambda$  Bootis stars, but not around all. Moreover the presence of gas *and* dust is only observed in one  $\lambda$  Bootis star unambiguously, HD 221756. Table 1 gives an overview of the detection of dust and/or gas around  $\lambda$  Bootis stars. If the material is confined in a disk coplanar with the star, only a fraction of the stars will show narrow absorption features and/or shell characteristics, namely those, where the star is seen nearly equator-on. On the other hand at least the more distant  $\lambda$  Bootis stars beyond the Local Bubble,  $d > 100$  pc, are expected to show interstellar absorption features.

### 3. Overall strategy and general remarks

The well established  $\lambda$  Bootis stars were taken from the list of Gray & Corbally (1998) and Paunzen (2001) with the exception of apparent spectroscopic binary systems (e.g. HD 64491, HD 141851 and HD 148638). In total, the list comprises of 65 objects. We have explicitly rejected any spurious objects. King (1994) has used the first catalogue of  $\lambda$  Bootis candidates from Renson et al. (1990) for his target selection including more than 100 objects. At least 50% of this sample was already recognized as being misclassified and several new  $\lambda$  Bootis type objects were discovered since then (Faraggiana & Bonifacio 1999, Paunzen 2001). A one-to-one comparison with the work of King (1994) is therefore not straightforward.

The literature was searched for measurements of well established  $\lambda$  Bootis type objects red-ward of 7000Å (approximate Johnson *R*). A blackbody radiation curve follows a standard ATLAS9 model very well within this spectral region. The *same* blackbody radiation curve for a temperature of 8500 K was used for all program stars. This curve is shifted by a constant for the individual objects mainly due to the different distance and interstellar absorption and thus reddening.

All measurements were transformed to Jansky with the calibrations listed in the following sections. The results are listed in Table 2 where *italized* values are only *upper limits*.

Figures 1 and 2 show the fluxes for all objects with photometric measurements beyond 2.2  $\mu\text{m}$  (open circles denote upper limits) together with the blackbody radiation curves.

#### 3.1. Measurements up to 1.1 $\mu\text{m}$

For this work we have used two different photometric systems (13 color and Johnson *RI*) taken from the General Catalogue of Photometric Data (GCPD; <http://obswww.unige.ch/gcpd/>) as well as spectrophotometry given by Oke (1967). This data is not color corrected because all calibrations are derived relative to an A0 V star (or Vega) with an effective temperature close to our program stars. The listed (e.g. Johnson & Mitchell 1975) color corrections are indeed close to zero. The observed magnitudes were directly converted into fluxes using the calibrations by Johnson & Mitchell (1975; 13 color system), Beckwith et al. (1976; Johnson *RI*) and Oke & Gunn (1983; spectrophotometry).

The absolute values sometimes differ which is probably caused by the contribution of Paschen lines in the relevant spectral domain.

#### 3.2. Johnson *JHKLM* photometry

Most of the data are taken from the 2 micron survey (Skrutskie et al. 1997) which lists *JHK* colors and their calibration. The other data (Baruch et al. 1983, Oudmaijer et al. 2001, GCPD) were calibrated using the values from Bessell & Brett (1988). Both sources take an A0 V star as standard. The measurements follow the blackbody radiation curve very well.

Gerbaldi (1991) presented *JHK* photometry for 25 candidate  $\lambda$  Bootis type objects. Unfortunately, instead of individual photometric magnitudes, calibrated spectral types are listed derived from  $(V - K)$  and  $(J - K)$  values. Hence, we were not able to include this data.

#### 3.3. IRAS photometry

The results of the IRAS satellite have been extensively analyzed in the past (Cheng et al. 1992, King 1994). The data is extracted from the IRAS Point Source Catalogue Version 2 and Faint Source Catalogue. Measurements with positional offsets more than  $3\sigma$  from the optical source were neglected. Most of the data for 25, 60 and 100  $\mu\text{m}$  are only upper limits (King 1994) and determined by the high background within these passbands. Since we want to get “upper limits” for possible disks around these objects, an independent estimation of the expected background was performed. Schlegel et al. (1998) list maps of dust infrared emission for the 100  $\mu\text{m}$  band derived from the COBE/DIRBE and IRAS/ISSA mea-

**Table 3.** List of observations performed with the ISO-satellite for well established members of the  $\lambda$  Bootis group; the column “mode” denotes chopped (c) or staring (s) observations.

HD	Inst.	TDT number	Program	mode
319	PHT03	37501221	RSTENCEL	s
	PHT22	37501238	RSTENCEL	s
11413	PHT03	35302022	RSTENCEL	s
	PHT22	35302039	RSTENCEL	s
110411	PHT03	20201523	RSTENCEL	s
	PHT22	20201540	RSTENCEL	s
125162	PHT03	16500415	CWAELKEN	c
	PHT03	35101427	WWEISS	c
	SWS01	35101303	WWEISS	c
142703	PHT03	43100804	WWEISS	c
142994	PHT03	09000784	RSTENCEL	s
183324	PHT03	12800785	RSTENCEL	s
	PHT22	53400928	RSTENCEL	s
192640	PHT03	34700540	RSTENCEL	s
	PHT22	34700537	RSTENCEL	s
	PHT03	38101529	WWEISS	c
	SWS01	38101302	WWEISS	c
	SWS01	38101406	WWEISS	c
193256	PHT03	36902530	RSTENCEL	s
	PHT22	36902547	RSTENCEL	s
198160	PHT03	54601631	RSTENCEL	s
	PHT22	54601648	RSTENCEL	s
204041	PHT03	71101211	WWEISS	c
210111	PHT03	36902628	RSTENCEL	s
	PHT22	36902645	RSTENCEL	s
221756	PHT03	38201729	RSTENCEL	s
	PHT03	41701332	WWEISS	c
	PHT22	38201746	RSTENCEL	s

surements. This consortium also presents maps for  $60\mu\text{m}$  (<http://astron.berkeley.edu/dust/>). These maps are used to derive a predicted background signal for a given galactical longitude and latitude which is then subtracted from the IRAS 60 and  $100\mu\text{m}$  measurements. The remaining upper limits for the  $60\mu\text{m}$  band are typically less than 0.1 Jansky whereas the values for the  $100\mu\text{m}$  band are slightly higher. Such corrected values are still upper limits and not apparent detections of fluxes from the targets themselves.

As a last step, the fluxes are color corrected using a 10000 K blackbody radiation (IRAS Explanatory Supplement VI.C.6). This has to be done because the absolute fluxes are not derived by using an A0 V standard star but by an internal calibration lamp (as for ISO).

### 3.4. ISO photometry

In this section we present the multifilter photometric observations for  $\lambda$  Bootis stars from the ISO satellite. The results of our program (WWEISS\_LBODISK) and the group of C. Waelkens (one measurement for HD 125162; CWAELKEN\_VEGASTAR) have not been published be-

**Table 4.** List of identified H I lines for the ISO-SWS spectra of HD 125162 and HD 192640 (Fig. 3) with the transition  $i \rightarrow j$

$\lambda$ [ $\mu\text{m}$ ]	i	j	$\lambda$ [ $\mu\text{m}$ ]	i	j	$\lambda$ [ $\mu\text{m}$ ]	i	j
2.526	5	16	2.675	5	13	3.297	5	9
2.564	5	15	2.758	5	12	3.741	5	8
2.613	5	14	2.873	5	11	3.749	6	17
2.626	4	6	3.039	5	10	3.819	6	16

fore. Fajardo-Acosta et al. (1999) presented the results of their working group (RSTENCEL\_VEGADIS7) which was partly focussed on the group of  $\lambda$  Bootis stars. They only list fluxes for HD 11413, HD 110411 and HD 192640 which were reduced with the PIA software (V6.3).

There are two different modes of ISO observations:

- chopped observations: the target and sky background is measured four times separately.
- staring observations: the measurements are made once at the target and once at the sky background. The ISO consortium soon realized that this mode was not very stable.

However, we treat both modes as having equal quality because we are not able to give any reasonable weights based on physical grounds. All data were newly reduced with the PIA software (V9.1; Gabriel et al. 1997) which should yield better calibrations than before. The color correction was done according to Chapter C.3 of the ISOPHOT/PIA manual. Fajardo-Acosta et al. (1999) give a calibration of ISO data at 3.6, 11.5 and  $20\mu\text{m}$  in comparison with IRAS and ground-based measurements. We have checked these calibrations and found an excellent agreement with the data reduced with the new software. We also have to emphasize that no study for the validity of the calibration for the measurements of A-type stars in the 25, 60 and  $100\mu\text{m}$  passbands exist. For the few cases for which IRAS and ISO measurements in the relevant passbands are available, they are in excellent agreement. We are therefore confident that the results from the PIA software (V9.1) have at least the same quality as the corresponding IRAS measurements. Table 3 lists all used multifilter photometric as well as spectroscopic (Section 3.5) ISO observations.

### 3.5. ISO-SWS spectroscopy for HD 125162 and HD 192640

The ISO-SWS spectroscopy is well suited to find atomic emission lines of H I, and molecular lines, like  $\text{H}_2$  or CO. This would allow to put further constraints on the accretion scenario and the chemical composition of the circumstellar material.

SWS spectroscopy was carried out for two well established  $\lambda$  Bootis stars, the prototype HD 125162 and HD 192640. The observation log is listed in Table 3. The reductions are performed using the standard software as

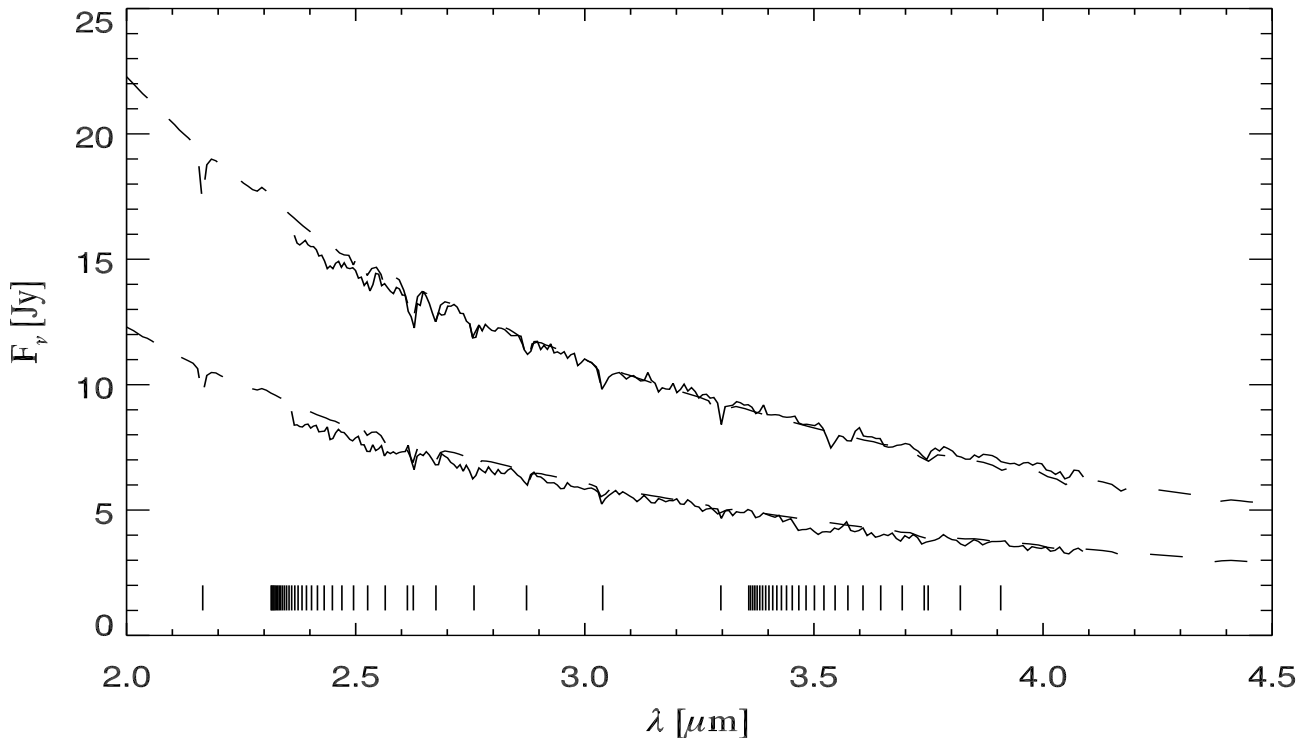


**Fig. 3.** ISO-SWS spectra for HD 125162 (upper lines) and HD 192640 (lower lines) compared to respective models of the stellar photosphere (ATLAS9). The H I lines are noted at the bottom.

provided by the ISO-consortium. The two individual spectra for HD 192640 were added. The signal-to-noise ratio of the spectra is about 15 to 20. For the wavelength region redder than  $4\ \mu\text{m}$  only upper limits due to the background noise can be given.

The absolute calibration of the spectra is very good. Figure 3 shows a comparison with theoretical ATLAS9 models (Kurucz 1992) using the following stellar parameters and distances (Stürenburg 1993, Heiter et al. 1998, Paunzen et al. 2002):  $T_{\text{eff}} = 9000\ \text{K}$ ,  $\log g = 4.0\ \text{dex}$ ,  $d = 30\ \text{pc}$  for HD 125162 and  $T_{\text{eff}} = 8000\ \text{K}$ ,  $\log g = 4.0\ \text{dex}$ ,  $d = 41\ \text{pc}$  for HD 192640. Because of the rather low signal-to-noise ratios of the spectra, an error of  $\pm 250\ \text{K}$  for the effective temperature and  $\pm 0.15\ \text{dex}$  for the surface gravity does not affect the conclusions.

From the spectra themselves, several H I lines (mainly the Pfund series) are identified. Table 4 lists the identified lines which are noted at the bottom of Fig. 3. The theoretical spectra were smoothed to a resolution corresponding to the SWS spectra in order to measure the equivalent widths of the hydrogen lines. Assuming a typical error of 1 and  $2.5\ \text{\AA}$  (taking also into account the difficulties of normalization) for the synthetic and the observed spectra respectively, no emission was found for the two  $\lambda$  Bootis stars (Fig. 4) within the error limits. This means that the observed H I lines are of pure stellar origin ruling out an

active accretion disk (as found for some Herbig Ae/Be stars) around these objects.

### 3.6. (Sub)millimeter observations at the Heinrich-Hertz-Telescope (HHT)

We have also observed five members of the  $\lambda$  Bootis group at (sub)millimeter wavelengths, in order to find signs of cold dust. The CO (2 – 1) line at 238.538 GHz was chosen, because it traces the molecular gas on excitation conditions characteristic for both the circumstellar and interstellar environment. Rentzsch-Holm et al. (1998) show that CO is not photodissociated in the circumstellar environment of stars with effective temperatures below 9000 K. We have selected five well established  $\lambda$  Bootis stars with effective temperatures below 9000 K where signs of gas and/or dust have already been detected: HD 31295, HD 74873, HD 125162, HD 192640, and HD 221756.

The observations were made at the Heinrich-Hertz-Telescope (Baars et al. 1999) on Mt. Graham, Arizona, in November 2000. We used the MPIfR 19 element bolometer array, that is sensitive at a spectral-response weighted frequency of 347 GHz with 110 GHz bandwidth. The array elements were calibrated by observations of the planets (Mars and Uranus were used as primary calibration sources). For the spectral line observations, a facility

**Table 5.** Stellar parameters and characteristics of the infrared excess: effective temperature  $T_{\text{eff}}$ , stellar luminosity  $L_*/L_\odot$ , stellar radius  $R_*/R_\odot$  and distance  $d$  are taken from Paunzen et al. (2002) and the spectral type from Gray & Corbally (1993). The characteristic dust temperature  $T_{\text{dust}}$  and fractional dust luminosity  $L_{\text{IR}}/L_*$  are deduced from the fits, while the radiative equilibrium distance  $r_{\text{dust}}$  is derived from Eq.(2).

HD	Sp. Type	$T_{\text{eff}}/\text{K}$	$L_*/L_\odot$	$R_*/R_\odot$	$d/\text{pc}$	$T_{\text{dust}}$	$r_{\text{dust}}/\text{AU}$	$L_{\text{IR}}/L_*$	$r_{\text{dust}}^{\text{ISM}}/\text{AU}$
110411 <sup>(a)</sup>	A0 Va ( $\lambda$ Boo)	8930	16.59	1.71	37.0	145	11.3	$1.7 \times 10^{-4}$	330
110411 <sup>(b)</sup>	A0 Va ( $\lambda$ Boo)	8930	16.59	1.71	37.0	116	17.7	$4.2 \times 10^{-5}$	609
125162	A0 Va $\lambda$ Boo	8720	19.05	1.92	30.0	70	51.3	$2.2 \times 10^{-5}$	2570
198160	A2 Vann wk $\lambda$ 4481	7870	22.91	2.58	73.0	130	16.0	$3.2 \times 10^{-4}$	476
210111	kA2hA7mA2Vas $\lambda$ Boo	7550	16.98	2.41	79.0	200	6.0	$4.3 \times 10^{-4}$	121

(a) fit to ISO fluxes

(b) fit to IRAS fluxes

215 – 275 GHz SIS receiver from Steward Observatory was used. Spectra were derived using a filterbank with 250 kHz channel spacing. The spectral line observations achieved a mean system temperature of 356 K (ranging between 303 and 435 K). For both line and continuum observations, the wobbler was used to remove the atmospheric emission, with 100'' and 200'' beam throw (the latter corresponds to the maximum beam separation of the array's elements), respectively. The beam sizes are 31'' for the CO spectroscopy and 21'' for the 347 GHz photometry.

The results are summarized in Table 6. No source was detected in the continuum, only one in the CO (2 – 1) line, which origin is unclear. Here are the results for the individual objects in more details:

*HD 31295* and *HD 74873*: Only 347 GHz photometry, but no detection. *HD 125162*: The source was observed in the CO line, but not detected.

*HD 192640*: The source was observed in the 347 GHz continuum and the CO line. The continuum of the source was not detected. A Gaussian fit to the CO line yields a system velocity of  $4.36 \text{ km s}^{-1}$  and a linewidth of  $1.66 \text{ km s}^{-1}$  (FWHM). However, a contamination by emission in the off-beam at  $-5.2 \text{ km s}^{-1}$  suggests extended CO emission of interstellar rather than circumstellar origin. This suggestion has been confirmed by an incomplete map peaking at offsets of  $\Delta\alpha = -65''$  and  $\Delta\delta = -152''$ . The CO flux and line area within the telescope's beam, at the source position, are  $11.4 \text{ Jy}$  and  $20.2 \text{ Jy km s}^{-1}$ , respectively. This emission is dominated by extended interstellar material. Dame et al. (1987) and Uyaniker et al. (2001) investigated survey data of the infrared, H I and CO emission in the relevant area. They conclude that the Orion local spiral arm is seen tangential towards the Cygnus region. This results in intense radio emission with a complex morphology. Discrete CO structures are seen at velocities between  $-10$  and  $+10 \text{ km s}^{-1}$  whereas large scale diffuse CO emission exists at velocities smaller than  $-12 \text{ km s}^{-1}$ .

*HD 221756*: Only CO spectroscopy, but no detection.

**Table 6.** Results of (sub)millimeter observations at the HHT.

HD	point source sensitivity [Jy]	
	CO(2-1) (238.5 GHz)	continuum (347 GHz)
125162	0.71	–
192640	1.87	0.017
221756	2.41	–
31295	–	0.013
74873	–	0.012

## 4. Results

In the literature, three well established  $\lambda$  Bootis stars with an apparent infrared excess were reported: HD 31295, HD 110411 and HD 125162 (see Section 2.1). Furthermore, a tentative detection for HD 11413 and HD 192640 was listed by Fajardo-Acosta et al. (1999). From our investigation, we are able to confirm the previous findings for HD 31295, HD 110411 and HD 125162. In addition, an infrared excess for HD 74873, HD 198160, HD 210111 and HD 221756 was found. This result is based on only one measurement at  $60 \mu\text{m}$  for HD 210111 and HD 221756 as well as  $25 \mu\text{m}$  for HD 74873 which makes a further investigation of the dust properties impossible.

We are not able to support the results for HD 11413 and HD 192640 as reported by Fajardo-Acosta et al. (1999). The ISO measurements for HD 192640 at 20 and  $25 \mu\text{m}$  are 0.19(13) and 0.20(28) Jy, respectively whereas the upper limit from the IRAS photometry at  $25 \mu\text{m}$  is 0.18 Jy (Table 2). The ISO measurements for HD 11413 at  $60 \mu\text{m}$  of 0.52(18) Jy is not in line with the upper limit of the IRAS value (0.13 Jy). This clearly calls for further measurements with higher sensitivity to to check the presence of an infrared excess for both objects.

Furthermore, we deduced the percentage of infrared measurements for well established  $\lambda$  Bootis stars redward of  $20 \mu\text{m}$  and the ratio of objects with infrared excesses. Table 2 includes 26 stars from which 11 have only upper limits, two are doubtful cases and 7 show no sign of an

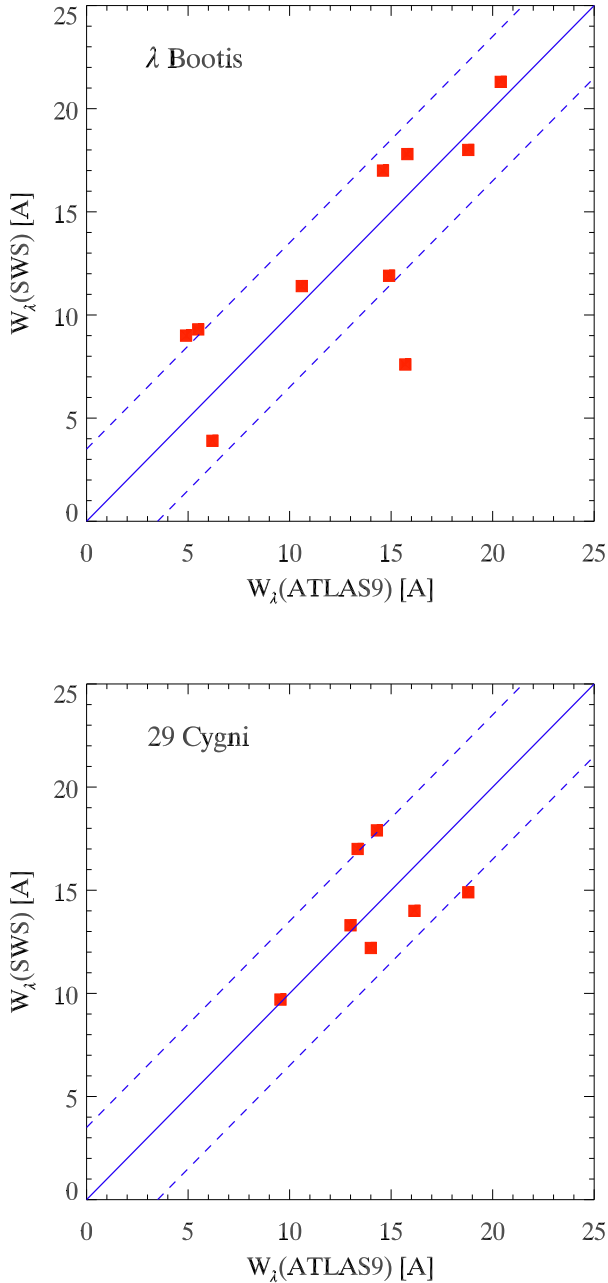


**Fig. 4.** Comparison of the equivalent widths of the H I lines from ATLAS9 models and the observed SWS spectra for HD 125162 (upper panel) and HD 192640 (lower panel). The dotted lines indicate the error due to the low signal-to-noise ratio and difficulties due to the normalization.

infrared excess. Hence, 23% of the  $\lambda$  Bootis stars show an infrared excess.

#### 4.1. Models of Infrared Excesses

For four stars in our sample, namely HD 110411, HD 125162, HD 198160 and HD 210111, the infrared excess

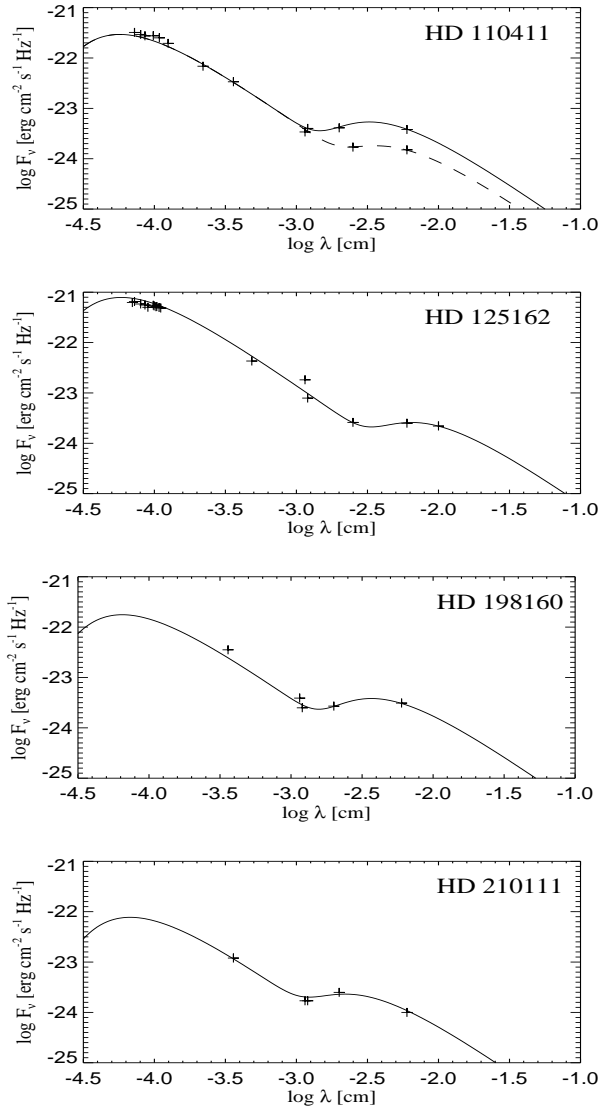


**Fig. 5.** Spectral energy distribution for well established  $\lambda$  Bootis stars with a detected infrared excess; the values for the latter were taken from Table 5. The full line for HD 110411 fits the ISO data whereas the dotted line fits the IRAS data.

is detected at two wavelengths. Any detailed modelling of the excess emission making use of more than two free parameters would be an overinterpretation of the data. Hence, we restrict ourselves to simply use a black body temperature  $T_{\text{dust}}$  and solid angle  $\Omega$  to fit the infrared excess of these four stars

$$F_{\text{dust}} = B_{\nu}(T_{\text{dust}})\Omega \quad \text{erg cm}^{-2} \text{ s}^{-1} \text{ Hz}^{-1}. \quad (1)$$

The total flux is given by adding the stellar flux and the infrared excess flux. From this fit, we obtain a characteristic dust temperature. Assuming large black body dust grains and radiative equilibrium, we can obtain the dis-

tance  $r_{\text{dust}}$  from the star at which the dust is heated to this temperature (Backman & Paresce 1993)

$$T_{\text{dust}} = 278 \left( \frac{L_*}{L_\odot} \right)^{0.2} \left( \frac{r}{\text{AU}} \right)^{-0.5} \text{ K} . \quad (2)$$

Moreover, we characterize the infrared excess in terms of the fractional dust luminosity  $L_{\text{IR}}/L_*$ , which is a measure of the optical thickness of the dust around the star.

Table 5 summarizes the results obtained from the infrared excess of the stars whereas Fig. 5 shows it graphically. The stellar parameters are taken from Paunzen et al. (2002) and the stellar radius is calculated from the effective temperature and luminosity of each star. In the case of HD 110411, IRAS gave systematically lower fluxes compared to ISO. Hence, we fitted the data separately. Fajardo-Acosta et al. (1999) used a combination of the IRAS 12 and 25  $\mu\text{m}$  fluxes and the ISO 11.5 and 20  $\mu\text{m}$  fluxes and fitted the infrared excess using a 190 K blackbody. They obtained a fractional dust luminosity of  $5 \times 10^{-5}$ . We have now an additional flux determination at 60  $\mu\text{m}$  and obtain a dust temperature of 145 K and a fractional dust luminosity of  $1.7 \times 10^{-4}$  from the ISO data.

Vega-type stars have typical fractional dust luminosities in the range  $10^{-6}$  to  $10^{-3}$  and characteristic dust temperatures below 100 K (Backman & Gillett 1987). Vega itself has a fractional luminosity of  $1.5 \times 10^{-5}$  and a dust temperature of 74 K, while  $\beta$  Pictoris has  $L_{\text{IR}}/L_* = 2.4 \times 10^{-3}$  and  $T_{\text{dust}} = 106$  K. The fractional dust luminosities derived for the four  $\lambda$  Bootis stars are of the same order as those of typical Vega-type stars, but the dust temperatures are often in excess of 100 K.

The dust around these four  $\lambda$  Bootis stars is typically located in the planet forming regions, 6 to 50 AU, but the nature of this dust remains unknown. From the present observations, we cannot conclude whether the dust is confined to a disk or distributed spherically around the stars. Since we lack detailed infrared spectroscopy at long wavelength ( $\lambda > 10\mu\text{m}$ ), nothing is known about the composition and size of these dust grains.

In a different paper, Kamp & Paunzen (2002) speculated that normal stars are turned for some time into  $\lambda$  Bootis stars by their passage through a diffuse interstellar cloud. In order to elaborate on this, we calculate the radiative equilibrium radii of typical ISM grains from Backman & Paresce (1993)

$$T_{\text{dust}} = 636 \left( \frac{L_*}{L_\odot} \right)^{\frac{2}{11}} \left( \frac{r}{\text{AU}} \right)^{-\frac{4}{11}} \left( \frac{T_*}{T_\odot} \right)^{\frac{3}{11}} \text{ K} , \quad (3)$$

where  $T_\odot$  is 5770 K and present them also in Table 5. The resulting radii are of the same order as the avoidance radii of dust grains, that is the radius of closest approach for ISM dust grains subject to the stellar radiation pressure. In this case the infrared excess would be caused by the dust grains of the diffuse ISM cloud as they approach the star and are repelled by its radiation pressure.

## 5. Conclusions

From the literature (King 1994, Fajardo-Acosta et al. 1999) it is already clear that 1) only very few  $\lambda$  Bootis members were detected in the IR and 2) even less objects show infrared excesses.

We present in this paper all available data for members of the  $\lambda$  Bootis group in the wavelength region beyond 7000 Å. The data include spectrophotometry, Johnson *RJHKLM* and 13-color photometry as well as IRAS and ISO measurements. All the data are homogeneously reduced and transformed into a standard system given in units of Jansky. In total, measurements for 34 (26 with data redward of 20  $\mu\text{m}$ ) well established  $\lambda$  Bootis stars are available. From those 26 objects, 6 show an infrared excess and 2 doubtful detections resulting in a percentage of 23%.

For four stars the infrared excess was detected at two different wavelengths allows to fit the data by a simple model. The derived dust temperatures lie between 70 and 200 K and the fractional dust luminosities range from  $2.2 \times 10^{-5}$  to  $4.3 \times 10^{-4}$ . These values are comparable with those found for Vega-type objects. While large black body grains indicate an origin of the IS emission in the planet forming region, small IS dust grains point towards much larger distances (a few hundred to a few thousand AU) from the star.

ISO-SWS spectroscopy for HD 125162 and HD 192640 resulted in the detection of pure stellar H I lines ruling out an active accretion disk around these objects.

Furthermore, a search for the CO (2–1) line at 238.538 GHz and continuum observations at 347 GHz of three  $\lambda$  Bootis stars yield only upper limits.

Our results clearly show that at least 23% of the  $\lambda$  Bootis stars have circumstellar or interstellar material around them. From the data summarized in this paper we infer that the presence of gas and dust around the stars is not correlated. However, to draw firm conclusions, more sensitive IR measurements are needed to be able to detect the stellar photosphere and thus exclude even the presence of weak dust emission. In addition, we would need a dedicated high resolution, high signal to noise survey for CS lines in  $\lambda$  Bootis stars to detect gas in the stellar surrounding.

*Acknowledgements.* We appreciate the assistance of the HHT staff and especially thank Maria Messineo for her help with the HHT observations. We would like to thank our referee, Dr. Turcotte for helpful comments. This work benefitted from the Fonds zur Förderung der wissenschaftlichen Forschung, project P14984. Use was made of the SIMBAD database, operated at CDS, Strasbourg, France and the GCPD database, operated at the Institute of Astronomy of the University of Lausanne. The ISOPHOT data presented in this paper were reduced using PIA, which is a joint development by the ESA Astrophysics Division and the ISOPHOT Consortium with the collaboration of the Infrared Processing and Analysis Center (IPAC). Contributing ISOPHOT Consortium institutes are DIAS, RAL, AIP, MPIK, and MPIA. The ISO Spectral Analysis Package (ISAP) is a joint development by the LWS

and SWS Instrument Teams and Data Centers. Contributing institutes are CESR, IAS, IPAC, MPE, RAL and SRON.

## References

- Abt, H.A., & Moyd, K.I., 1973, *ApJ*, 182, 809
- Andrievsky, S.M. 1997, *A&A*, 321, 838
- Andrievsky, S.M., & Paunzen, E. 2000, *MNRAS*, 313, 547
- Andrillat, Y., Jaschek, C., Jaschek, M. 1995, *A&A*, 299, 493
- Aumann, H.H. 1985, *PASP*, 97, 885
- Aumann, H.H. 1991, In: *The Infrared Spectral Region of Stars*, C. Jaschek, & Y. Andrillat (eds.), Cambridge University Press, Cambridge, p. 363
- Aumann, H.H., Gillett, F.C., Beichman, C.A., De Jong, T., Houck, J.R., et al. 1984, *ApJ*, 278, L23
- Baars, J.W.M., Martin, R.N., Mangum, J.G., McMullin, J.P., Peters, W.L. 1999, *PASP*, 111, 627
- Backman, D.E. & Gillett, F.C. 1987, *Cool Stars, Stellar Systems and the Sun*, Proceedings of the Fifth Cambridge Workshop held in Boulder, Colo., 8-11 Jul. 1987. Lecture Notes in Physics, J.L. Linsky and R.E. Stencel (eds.), Vol. 291, Springer-Verlag, Berlin, p.340
- Backman, D.E. & Paresce, F. 1993, In: *Protostars and Planets III*, E. Levy, & J. Lunine (eds.), The University of Arizona Press, p. 1253
- Baruch, J.E.F., Griffiths, W.K., Groote, D., et al. 1983, *MNRAS*, 202, 691
- Beckwith, S., Evans, N.J., Becklin, E.E., Neugebauer, G. 1976, *ApJ*, 208, 390
- Bessell, M.S., & Brett J.M. 1988, *PASP*, 100, 1134
- Bohlender, D.A., Gonzalez, J.F., Matthews, J.M. 1999, *A&A*, 350, 553
- Bohlender, D.A., & Walker, G.A.H. 1994, *MNRAS*, 266, 891
- Charbonneau, P. 1993, *ApJ*, 405, 720
- Cheng, K.P., Bruhweiler, F.C., Kondo, Y., Grady, C.A. 1992, *ApJ*, 396, L83
- Ciardi, D.R., van Belle, G.T., Akeson, R.L., Thompson, R.R., Lada, E.A., Howell, S.B. 2001, *ApJ*, 559, 1147
- Crutcher, R.V. 1982, *ApJ*, 254, 82
- Dame, T.M., Ungerechts, H., Cohen, R.S., et al., 1987, *ApJ*, 322, 706
- Dunkin, S.K., Barlow, M.J., Ryan, S.G. 1997, *MNRAS*, 286, 604
- Fajardo-Acosta, S.B., Stencel, R.E., Backman, D.E., Thakur, N. 1999, *ApJ*, 520, 215
- Faraggiana, R., & Bonifacio, P. 1999, *A&A*, 349, 521
- Faraggiana, R., Gerbaldi, M., Böhm, C. 1990, *A&A*, 235, 311
- Faraggiana, R., Gerbaldi, M., Bonifacio, P., François, P., 2001, *A&A*, 376, 586
- Faraggiana, R., Gerbaldi, M., Burnage, R. 1997, *A&A*, 318, L21
- Gabriel, C., Acosta-Pulido, J., Heinrichsen, I., Morris, H., Tai, W.-M. 1997, In: *Astronomical Data Analysis Software and Systems (ADASS) VI*, G. Hunt & H.E. Payne (eds.), ASP Conf. Ser. Vol. 125, 108
- Gerbaldi, M. 1991, In: *The Infrared Spectral Region of Stars*, C. Jaschek & Y. Andrillat (eds.), Cambridge University Press, Cambridge, p. 307
- Grady, C.A., Perez, M.R., Talavera, A., et al. 1996, *ApJ*, 471, 49
- Gray, R.O. 1988, *AJ*, 95, 220
- Gray, R.O., & Corbally, C.J. 1993, *AJ*, 106, 632
- Gray, R.O., & Corbally, C.J. 1998, *AJ*, 116, 2530
- Gray, R.O., & Corbally, C.J. 2002, *AJ*, 124, 989
- Gray, R.O., & Garrison, R.F. 1987, *ApJS*, 65, 581
- Gulliver, A.F., Hill, G., Adelman, S.J. 1994, *ApJ*, 429, L81
- Habing, H.J., Dominik, C., Jourdain de Muizon, M. et al. 2001, *A&A*, 365, 545
- Hauck, B., Ballereau, D., Chauville, J. 1995, *A&AS*, 109, 505
- Hauck, B., Ballereau, D., Chauville, J. 1998, *A&AS*, 128, 429
- Heinrichsen, I., Walker, H.J., Klaas, U. 1998, *MNRAS*, 293, L78
- Heiter, U. 2002, *A&A*, 381, 959
- Heiter, U., Kupka, F., Paunzen, E., Weiss, W.W., Gelbmann, M. 1998, *A&A*, 335, 1009
- Holland, W.S., Greaves, J.S., Zuckerman, B. et al. 1998, *Nature*, 392, 788
- Holweger, H., & Stürenburg, S. 1991, *A&A*, 252, 255
- Holweger, H., & Rentzsch-Holm, I. 1995, *A&A*, 303, 819
- Holweger, H., Hempel, M., Kamp, I. 1999, *A&A*, 350, 603
- Holweger, H., Hempel, M., van Thiel, T., Kaufer, A. 1997, *A&A*, 320, L49
- Iliev, I.Kh., Paunzen, E., Barzova, I.S., et al., 2002, *A&A*, 381, 914
- Jaschek, C., Jaschek, M. 1987, *The Classification of Stars*, Cambridge University Press, Cambridge
- Jaschek, M., Jaschek, C., Andrillat, Y. 1988, *A&AS*, 72, 505
- Johnson, H.L., & Mitchell, R.I. 1975, *RMxAA*, 1, 299
- Kamp, I., Hempel, M., Holweger, H. 2002, *A&A*, 388, 978
- Kamp, I., & Paunzen, E. 2002, *MNRAS*, 335, L45
- Kessler, M.F., Steinz, J.A., Anderegg, M.E., et al. 1996, *A&A*, 315, 27
- King, J.R. 1994, *MNRAS*, 269, 209
- Kurucz, R.L. 1992, *Rev. Mex. Astron. Astrof.*, 23, 181
- Lagrange-Henri, A.M., Beust, H., Ferlet, R., Hobbs, L.M., Vidal-Madjar, A. 1990, *A&A*, 227, L13
- Marchetti, E., Faraggiana, R., Bonifacio, P. 2001, *A&A*, 370, 524
- McAlister, H.A., Mason, B.D., Hartkopf, W.I., Shara, M.M. 1993, *AJ*, 106, 1639
- Michaud, G., & Charland, Y. 1986, *ApJ*, 311, 326
- Oudmaijer, R.D., Palacios, J., Eiroa, C., et al. 2001, *A&A*, 379, 564
- Oke, J.B. 1967, *ApJ*, 150, 513
- Oke, J.B., & Gunn, J.E. 1983, *ApJ*, 266, 713
- Paunzen, E. 2001, *A&A*, 373, 633
- Paunzen, E., Iliev, I.Kh., Kamp, I., Barzova, I.S. 2002, *MNRAS*, 336, 1030
- Renson, P., Faraggiana, R., Böhm, C. 1990, *Bull. Inform. CDS*, 38, 137
- Rentzsch-Holm, I., Holweger, H., Bertoldi, F. 1998, In: *Star Formation with the Infrared Space Observatory*, J. Yun & R. Liseau (eds.), ASP Conf. Ser. Vol. 132, 275
- Sadakane, K., & Nishida, M. 1986, *PASP*, 98, 685
- Schlegel, D.J., Finkbeiner, D.P., Davis, M. 1998, *ApJ*, 500, 525
- Skrutskie, M., Schneider, S.E., Stiening, R. 1997, In: *The Impact of Large Scale Near-IR Sky Surveys*, F. Garzon et al. (eds.), Dordrecht, Kluwer Academic Publishing Company, p. 25
- Smith, B.A., & Terrile, R.J. 1984, *Science*, 226, 1421
- Spitzer, L. 1968, *Diffuse Matter in Space*, Interscience Publ., New York
- Stürenburg, S. 1993, *A&A*, 277, 139
- Turcotte, S. 2002, *ApJ*, 573, L129
- Turcotte, S., & Charbonneau, P. 1993, *ApJ*, 413, 376
- Uyaniker, B., Fürst, E., Reich, W., Aschenbach, B., Wielebinski, R. 2001, *A&A*, 371, 675

Venn, K.A., & Lambert, D.L. 1990, ApJ, 363, 234

Waters, L.B.F.M., Trams, N.R., Waelkens, C. 1992, A&A, 262,  
L37